Articles

Heterogeneous Nucleation of ZnO Using Gelatin as the Organic Matrix

Luciana Pitta Bauermann,*,† Aránzazu del Campo,‡ Joachim Bill,† and Fritz Aldinger†

Pulvermetallurgisches Laboratorium and Department Arzt, Max-Planck-Institut für Metallforschung and Institut für Nichtmetallische Anorganische Materialien, Universität Stuttgart, Heisenbergstr. 3, D-70569 Stuttgart, Germany

Received October 21, 2005. Revised Manuscript Received February 9, 2006

The presence of dissolved gelatin in the sol state during the crystallization of ZnO has a substantial influence on its morphology. The gelatin behaves as a matrix where the ZnO is heterogeneously nucleated. The experimental conditions used during crystallization are very mild consisting of a diluted aqueous buffered solution of zinc nitrate and gelatin at a pH close to neutral and 37 °C. This bio-friendly environment is essential for the integrity of the protein. In the absence of gelatin, nearly spherical ZnO nanoparticles of a diameter of about 20 nm were obtained. By the presence of dissolved gelatin at a concentration of 1.2 mg/mL, the morphology of ZnO is drastically changed to twinned hexagonal plates with (002) faces of about 460 nm diameter and 40 nm thick. Oxide materials with this shape are especially interesting for piezoelectric applications. A mechanism of nucleation and crystal growth is proposed.

Introduction

Biominerals are usually formed at the surface of organic templates (or matrixes).[1,2] These interactions between dissolved ions and specific surfaces affect not only the particle size and habit of nucleating crystals but also the stability of intermediate phases by dropping the activation energy required for the formation of specific crystal faces.[3] The organic templates nucleate the mineral by controlling its crystallographic orientation and growth, by imitating the lattice of a two-dimensional face, or by the stereochemistry of the functional groups at the interface.[4] Recent studies suggest that an epitaxial or geometrical match between macromolecules and crystalline faces does not occur. Instead, the charge density on the crystalline faces, and thus the electrostatic attraction, is alone sufficient for the heterogeneous nucleation.[5,6] There has been much effort in trying to elucidate the mechanism of proteins and other biomolecules on biomineralization.[7] Many in vitro studies have demonstrated the importance of proteins and peptides in controlling the nucleation and/or growth of crystals.[4,6,8−14] These were all publications where the gelatin, or collagen, was used as the organic matrix. Gelatin is the denaturation product of collagen, which is the major structural protein in the connective tissue of animal skin and bone. This protein is rather simple consisting of a highly repetitive sequence of amino acids $[(Gly)\text{-}X\text{-}Y]_n$, where Gly stands for glycine, X is often proline (Pro), and Y is hydroxyproline (Hyp).[15] Collagen is formed by three chains, over 1400 amino acids long, which wound together in a tight triple helix in the shape of a rope. Gelatin, on the other hand, consists of only one single chain of these sequenced amino acids and is promptly soluble in warm water. Several other biomolecules were also investigated by in vitro biomineralization.[16−19]

Proteins are not often employed on mineralization because of their complexity and the demand of extremely mild experimental conditions necessary to preserve their physical

* To whom correspondence should be addressed. E-mail: pitta@mf.mpg.de.
† Pulvermetallurgisches Laboratorium.
‡ Department Arzt.

(1) Dujardin, E.; Mann, S. *Adv. Mater.* **2002**, *14* (11), 775−788.
(2) Teng, H. H.; Dove, P. M. and DeYoreo, J. J. *Geochim. Cosmochim. Acta* **1999**, *63* (17), 2507−2512.
(3) Cölfen, H.; Mann, S. *Angew. Chem., Int. Ed.* **2003**, *42*, 2350−2365.
(4) Falini, G. *Int. J. Inorg. Mater.* **2000**, *2*, 455−461.
(5) Volkmer, D.; Fricke, M.; Gleiche, M.; Chi, L. *Mater. Sci. Eng., C* **2005**, *25* (2), 161−167.
(6) Coradin, T.; Bah, S.; Livage, J. *Colloids Surf., B* **2004**, *35*, 53−58.
(7) Silverman, L.; Boskey, A. L. *Calcif. Tissue Int.* **2004**, *75*, 494−501.
(8) Busch, S.; Schwarz, U.; Kniep, R. *Adv. Funct. Mater.* **2003**, *13* (3), 189−198.
(9) Göbel, C.; Simon, P.; Buder, J.; Tlatlik, H.; Kniep, R. *J. Mater. Chem.* **2004**, *14*, 2225−2230.
(10) Itoh, S.; Kikuchi, M.; Koyama, Y.; Matumoto, H. N.; Takakuda, K.; Shinomiya, K.; Tanaka, J. *Biomed. Mater. Eng.* **2005**, *15* (1−2), 29−41.
(11) Chang, M. C.; Ko, C.-C.; Douglas, W. H. *Biomaterials* **2003**, *24*, 3087−3094.
(12) Bigi, A.; Panzavolta, S.; Roveri, N. *Biomaterials* **1998**, *19*, 739−744.
(13) Grassmann, O.; Müller, G.; Lobmann, P. *Chem. Mater.* **2002**, *14*, 4530−4535.
(14) Shen, F. H.; Feng, Q. L.; Wang, C. M. *J. Cryst. Growth* **2002**, *242*, 239−244.
(15) Segtnan, V. H.; Isaksson, T. *Food Hydrocolloids* **2004**, *18*, 1−11.
(16) Belton, D.; Paine, G.; Patwardhan, S. V.; Perry, C. P. *J. Mater. Chem.* **2004**, *14*, 2231−2241.
(17) Kisailus, D.; Choi, J. H.; Weaver, J. C.; Yang, W.; Morse, D. E. *Adv. Mater.* **2005**, *17* (3), 314−318.
(18) Dickerson, M. B.; Naik, R. R.; Stone, M. O.; Cai, Y.; Sandhage, K. H. *Chem. Commun.* **2004**, *15*, 1776−1777.
(19) Lévêque, I.; Cusack, M.; Davis, S. A.; Mann, S. *Angew. Chem., Int. Ed.* **2004**, *43*, 885−888.

10.1021/cm052317+ CCC: $33.50
Published on Web 03/16/2006

and chemical properties. Good substitutes are synthetic polymers. They were used as additives modifying particle shapes, sizes, and crystal phases of ZnO.[20−25] Single-crystalline hexagonal disks and rings of ZnO with morphology very similar to the one introduced by us here were obtained using an oil−water microemulsion with surfactant in water with 1-butanol and $Zn(NO_3)_2$.[26] Also, trisodium citrate induces the formation of short ZnO hexagonal microrods with stacked-nanoplate structure.[27] These microrods appear to be formed in two halves, with upper and lower layers stacked together. The authors claimed that the trisodium citrate attaches on the Zn^{2+} (0001) surfaces through the COO^- and OH^- groups suppressing its growth along the ⟨001⟩ direction.

It is of primary importance to control the size, shape, and preferred orientation of ZnO nanostructures for tailoring its chemical and physical properties. We believe that, after overcoming the preliminary obstacles, proteins can work as unique additives because of their three-dimensional complexity. As far as we know, this is the first time that the crystallization of zinc oxide is reported in the presence of gelatin. It is important to mention that, with very few exceptions,[6] we have used a much lower concentration of gelatin (0.12 wt %) than other works dealing with the influence of this protein on the nucleation and growth of different minerals (about 10 wt %).[8,13] In our experimental conditions (gelatin concentration and temperature) the gelatin is found in the sol state dispersed mainly as random coils. The overlapping of chains which, above a certain concentration, is responsible for the gelation of the gelatin is predominantly absent.[28] Gelatin is found as a gel at a concentration typically higher than 1 wt %.[28] The heterogeneous nucleation of ZnO using other proteins was also investigated.[29] But the ZnO acquired such special morphology as reported here only when gelatin was used. We suppose the interesting characteristic of the gelatin is its elongated structure, which is unusual among proteins.

Experimental Section

ZnO Crystallization. The ZnO was prepared by adding a specific volume of aqueous solution of 500 mM $Zn(NO_3)_2(H_2O)_6$ to a final concentration of 20 mM in 30 mM buffer tris(hydroxymethyl)aminomethane (TRIZMA) buffer at pH 8. TRIZMA buffer was prepared by dissolving 1.842 g/L Trizma HCl and 2.22 g/L Trizma base in deionized water. The buffer solution contained gelatin type B from bovine skin (about 225 Bloom and molecular weight of 50 kDa) dissolved in a concentration of 1.2 mg/mL. The reaction occurs at 37 °C during 4 h. The precipitate was then centrifuged and washed with deionized water at 37 °C and dried at 37 °C in air. The chemicals are reagent grade, purchased from Sigma Aldrich, and were used without further purification.

The ZnO crystallized in absence of gelatin followed the same procedure as above except for the dissolved gelatin added to the buffer.

Characterization of ZnO Particles. The ZnO particles were characterized using scanning electron microscopy (SEM), X-ray powder diffraction (XRD), and transmission electron microscopy (TEM).

ZnO was poured on silicon wafers and dried at room temperature using argon flow. The samples were sputtered with Pt/Pd before being analyzed by SEM (JEOL 6300F).

ZnO samples were ground with a standard silicon powder (Merck) for XRD (Siemens D5000 X-ray diffractometer, using filtered Cu Kα radiation over a 2θ range from 10° up to 80° with a step size of 0.02° and counting time of 10 s/step). The positions of the ZnO reflections were corrected on the basis of those of silicon.

For TEM characterization of the ZnO synthesized in the presence of gelatin, three methods of preparation were used: For the sample where the basal planes of the ZnO were parallel to the surface of the TEM holder, the crystals were simply ultrasonicated in ethanol and dispersed on Cu grids (Ted Pella, Inc., U.S.A.). To investigate the interior of the hexagonal crystals, they were cut by means of a focus ion beam (Dual Beam Nova 600 Nanolab) or embedded in resin and cut by microtoming. Energy-filtering transmission electron microscopy (EFTEM) was performed by the three-window method on a Zeiss 912 Omega energy-filtering microscope operating at 120 kV using the C K edge for the carbon mapping. Electron energy-loss spectroscopy (EELS) spectra were recorded in a VG STEM HB501 UX. A series of spectra were acquired along a line parallel to the ZnO−platelet normal. Composition profiles were extracted from these line scans.

Characterization of Gelatin. Zeta potential measurements were carried out in diluted suspensions using KNO_3 as the ionic background by a Zetasizer 3000 HSA (Malvern Instruments, Ltd., Malvern, U.K.).

Amino Funcionalization of the Silica Surface. The 10 × 26 mm silicon substrates (silicon p-type {001}, Wacker Siltronic) were soaked in piranha solution (H_2SO_4/H_2O_2, 5 parts to 1, respectively) overnight and then washed throughout with deionized water. A solution of 20 mg of aminopropyl(triethoxysilane)/mL deionized water (ABCR, Karlsruhe) was stirred for 30 min and filtered through a 0.2 μm filter. The silicon substrates were immersed into the prehydrolyzed solution for 1 h, washed with deionized water, and baked at 95°C under vacuum for 1 h.

Immobilization of Gelatin via Glutaraldehyde Coupling. The amine modified substrates were washed twice with coupling buffer of sodium chloride−sodium citrate (Aldrich) in deionized water (1 × SSC buffer at pH 7.3). They were immersed in a glutaraldehyde (Aldrich) solution in a concentration of 50 mg/mL in coupling buffer for 3 h at room temperature. The substrates were subsequently washed five times with coupling buffer to remove the excess of glutaraldehyde.

The aldehyde activated substrates were washed twice with phosphate buffered saline (PBS) at pH 7.2 (Aldrich) and immersed in a 0.55 mg/mL solution of gelatin in PBS at pH 7.2. The reaction was allowed to proceed at room temperature overnight. Subsequently, the substrates were washed to remove the uncoupled gelatin with PBS, first at pH 7.2 and then at pH 6.8. For the reduction of

(20) Taubert, A.; Palms, D.; Weiss, Ö.; Piccini, M. T.; Batchelder, D. N. *Chem. Mater.* **2002**, *14*, 2594−2601.
(21) Lin, Y.; Xie, J.; Wang, H.; Li, Y.; Chavez, C.; Lee, S. Y.; Foltyn, S. R.; Crooker, S. A.; Burrell, A. K.; McCleskey, T. M.; Jia, Q. X. *Thin Solid Films* **2005**, *492* (1−2), 101−104.
(22) Jin, C. F.; Yuan, X.; Ge, W. W.; Hong, J. M.; Xin, X. Q. *Nanotechnology* **2003**, *14*, 667−669.
(23) Wang, C.; Shen, E.; Wang, E.; Gao, L.; Kang, Z.; Tian, C.; Lan, Y.; Zhang, C. *Mater. Lett.* **2005**, *59* (23), 2867−2871.
(24) Tian, Z. R.; Voigt, J. A.; Liu, J.; McKenzie, B.; McDermott, M. J.; Rodriguez, M. A.; Konishi, H.; Xu, H. *Nat. Mater.* **2003**, *2*, 821−826.
(25) Liang, J.; Liu, J.; Xie, Q.; Bai, S.; Yu, W.; Qian, Y. *J. Phys. Chem. B* **2005**, *109*, 9463−9467.
(26) Li, F.; Ding, Y.; Gao, P.; Xin, X.; Wang, Z. L. *Angew. Chem.* **2004**, *116*, 5350−5354.
(27) Kuo, C.-L.; Kuo, T.-J.; Huang, M. H. *J. Phys. Chem. B* **2005**, *102* (43), 20115−20121.
(28) Bohidar, H. B.; Maity, S. *Eur. Polym. J.* **1998**, *34* (9), 1361−1370.
(29) Bauermann, L. P.; Bill, J.; Aldinger, F. Manuscript in preparation.

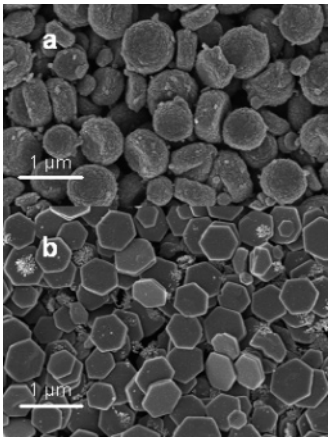

Figure 1. SEM images of ZnO particles synthesized in aqueous solution at 37 °C in pH 8 buffer for 4 h (a) without gelatin and (b) with 1.2 mg gelatin/mL. The insets are histograms displaying the particle size distributions of both ZnO types.

the imine bond, the substrates were immersed in PBS at pH 6.8 containing $NaBH_3CN$ (Aldrich; 20 mg/mL), and the reduction reaction took 4 h at room temperature. The supports were washed with PBS at pH 6.8 and immersed in PBS at pH 9.2 containing 15 mg of $NaBH_3CN$/mL at room temperature for 1 h to reduce all free carbonyl groups. Finally the substrate was immersed in 5 mM glycine dissolved in PBS at pH 7.2 and then washed and kept in PBS at pH 7.2.

Characterization of the Gelatin Film. Atomic force microscopy (AFM) measurements were recorded by a Digital Instruments Nanoscope IIIa applying the tapping mode with an etched silicon cantilever, Veeco. The thickness of the film was determined by carefully scratching the film with a sharp needle and measuring the depth of the scratch. The roughness was measured from areas of 2.5 × 2.5 μm^2 size.

Formation of the ZnO Film on Top of the Gelatin Film. The silicon substrates covered with a solution of gelatin were placed vertically in a chamber with 20 mM $Zn(NO_3)_2$ and 30 mM TRIZMA buffer, pH 8, at 37 °C for 4 h. The substrates were then washed thoroughly with deionized water and dried with argon flow.

Results and Discussion

The SEM images in Figure 1 show the extraordinary change in ZnO morphology by the presence of 1.2 mg of gelatin dissolved per 1 mL of buffer solution before the addition of zinc cations. The ZnO crystallized in the absence of gelatin (Figure 1a) consists of about 750 nm large polycrystalline agglomerates composed of about 20 nm large round-shaped nanoparticles. ZnO crystals synthesized in the presence of dissolved gelatin in the sol state are formed like twinned platelets of hexagonal-shaped crystals with diameters of about 460 nm (Figure 1b). The particle size distributions of the agglomerates shown in Figure 1a and the largest plane of ZnO illustrated in Figure 1b were realized by analyzing SEM images using the software Image Tool for Windows, version 3.00. The histograms are displayed in Figure 2. The use of a lower concentration of gelatin did not produce such regularly shaped ZnO crystals. On the other hand, if a much higher concentration of this protein was used, a gel was formed and no ZnO precipitated.

XRD measurements displayed in Figure 3 show that the ZnO has wurtzite structure when crystallized both with and

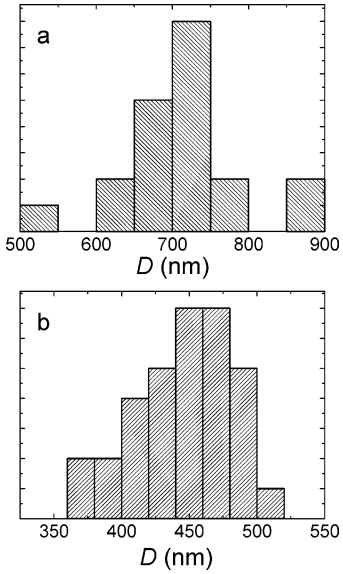

Figure 2. Histograms of particle size distributions of (a) the polycrystalline agglomerates displayed in Figure 1a and (b) the hexagonal plane of the crystallites shown in Figure 1b. The size of the particles was measured using the software Image Tool for Windows, version 3.00.

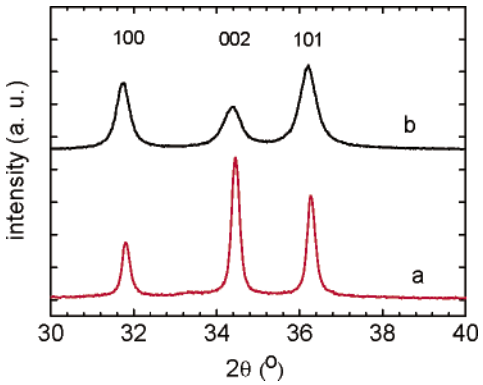

Figure 3. XRD spectra of ZnO particles synthesized in aqueous solution at 37 °C in pH 8 buffer for 4 h: (a) 1.2 mg gelatin/mL and (b) with no gelatin.

without gelatin. In the presence of dissolved gelatin there is an intensification of the peak (002) indicating a preferential growth perpendicular to *c* axis. ZnO with the ⟨002⟩ orientation normal to the substrate is especially attractive for piezoelectric applications.[30,31] This is also the most densely packed and thermodynamically favorable plane in the wurtzite structure.[30] The average diameter of the particle, *D*, was calculated for the ZnO crystallized in the absence of gelatin using the Scherrer equation,[32] $D = (K\lambda)/\beta(\cos\theta)$, on the reflections with $hkl = 100$, 002, and 101 (see Table 1), where *K* is the shape factor of the average crystallite (expected shape factor is 0.9), λ is the wavelength for the $K\alpha_1$ component of the employed copper radiation (1.540 56 Å), β is the full width at half-maximum of the diffraction line, and θ is the Bragg's angle. The size of the ZnO nanocrystallites formed in the absence of gelatin is calculated as about 20 nm. The Scherrer equation is not valid in the case of

(30) Park, S.-H. K.; Lee, Y. E. *J. Mater. Sci.* **2004**, *39*, 2195−2197.
(31) Gao, P. X.; Wang, Z. L. *J. Appl. Phys.* **2005**, *97*, 044304.
(32) Warren, B. E. *X-ray diffraction*; Addison-Wesley: Reading, MA, 1969.
(33) Massiot, D.; Fayon, F.; Capron, M.; King, I.; Calvé, S. L.; Alonso, B.; Durand, J.-O.; Bujoli, B.; Gan, Z.; Hoatson, G. *Magn. Reson. Chem.* **2002**, *40*, 70−76.

Table 1. Data Resulting from XRD Analysis of ZnO Synthesized at 37 °C without Gelatin[a]

	ZnO sample		
direction	(100)	(002)	(101)
2θ (deg)	31.74	34.38	36.20
β (deg)	0.38	0.54	0.49
D (nm)	22	15	17

[a] The average crystallite sizes D were calculated by applying the Scherrer equation[32] on the reflections with $hkl = 100$, 002, and 101. The value of the Bragg's angle, θ, and the full width at half-maximum, β, were measured using the DmFit program.[33]

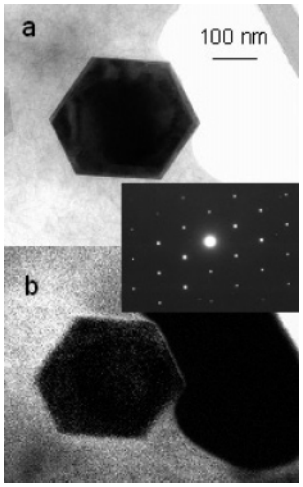

Figure 4. (a) Bright-field TEM image and (b) element mapping carbon (brighter contrast corresponds to higher concentration of carbon) of ZnO synthesized in aqueous solution at 37 °C in pH 8 buffer for 4 h in the presence of 1.2 mg gelatin/mL. The inset shows the electron diffraction pattern taken parallel to the platelet normal.

nonspherical crystals, like the ZnO crystallized in the presence of gelatin.

In an attempt to localize any presence of organic matrix on the ZnO crystals, elemental mapping of carbon using EFTEM was performed. Proteins are formed from amino acids, and so they are rich in carbon. The bright-field TEM image (Figure 4a) does not show defects in the single-crystalline material. Figure 4b shows a carbon map obtained by EFTEM. Brighter areas indicate higher concentrations of carbon (protein). The brightest part of the image corresponds to gelatin dissolved in the buffer solution. No organic material was observed adsorbed on the ZnO crystallite. The electron diffraction pattern taken parallel to the platelet normal (Figure 4, inset) confirms the single-crystal quality of the ZnO−gelatin crystals.

The crystals were then cut to investigate the possible organic matrix inside them. These cuts were done by two different methods: focus ion beam and microtoming with the slices examined using TEM. A TEM image of cross sections of ZnO cut by focus ion beam is displayed in Figure 5 revealing the existence of an intersection between the two platelets. The cross section of the ZnO was measured as 39 ± 4 nm thick, by using the software Image Tool for Windows. EELS line scans were recorded transversely to the crystal to measure the profile of the carbon concentration. These measurements were performed in many different ZnO crystals and were very reproducible. Figure 6a shows a TEM image of a sample prepared by focus ion beam, and Figure 6b shows the corresponding profile of the carbon concentration across the crystal. Outside the ZnO there is a high concentration of protein related to the gelatin dissolved in the buffer solution, as can be observed also in Figure 4b. The carbon concentration decreased inside the ZnO, as expected, and increased in the middle of the crystallite, where the junction of the platelets is. There is a localized region of carbon on the platelets intersection. Between the two platelets there is a thin layer of organic material of about 4−5 nm thickness.

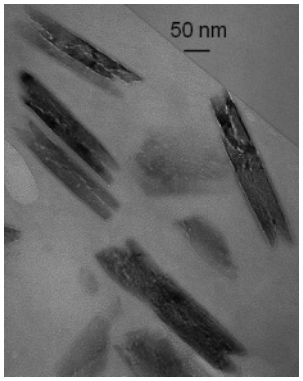

Figure 5. Dark-field TEM image of a cross section of ZnO synthesized in aqueous solution at 37 °C in pH 8 buffer for 4 h in the presence of 1.2 mg gelatin/mL cut by means of the focus ion beam.

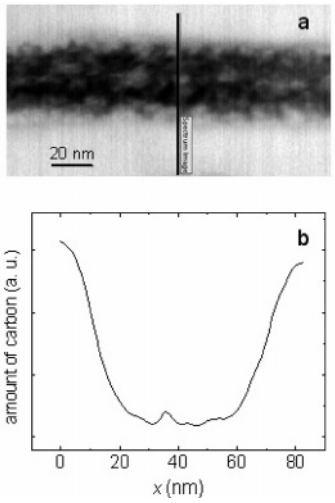

Figure 6. (a) Dark-field TEM image of a cross section of ZnO synthesized in aqueous solution at 37 °C in pH 8 buffer for 4 h in the presence of 1.2 mg gelatin/mL cut by means of the focus ion beam. The line scan is investigated from top to bottom. (b) Corresponding elemental map of carbon across the crystal.

The experimental value of the isoelectric point of gelatin is 6.6. So at the pH used in our experiments, about 8, this protein is slightly negatively charged. The nucleation mechanism proposed by us (Scheme 1) starts with the electrostatic attraction between the positively charged Zn^{2+}−water complex and the carboxylic groups of the negatively charged gelatin. With the gelatin concentration and temperature applied by us, the gelatin is in the sol state dispersed mainly as random coils. The ionic strength of the solution, which is increased by the addition of zinc ions, has very little effect on the gelation of the gelatin.[28] These random coils behave as organic matrixes holding many zinc cations on the negatively charged amino acids of the gelatin. The deprotonation of the aquo-complex is catalyzed by the buffer, which consumes the protons keeping the pH of the solution

Scheme 1. Heterogeneous Nucleation of ZnO on the Surface of Dissolved Gelatin[a]

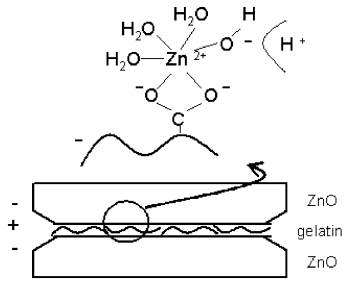

[a] There is an initial electrostatic attraction between the positively charged zinc aquo-complex and the carboxylic groups of the negatively charged gelatin. The growth of ZnO happens with the hydrolysis of the zinc aquo-complex and is catalyzed by the buffer consumption of protons.

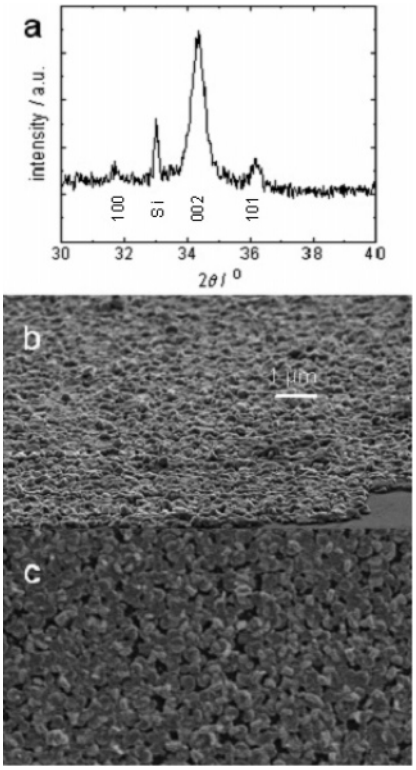

Figure 7. (a) XRD spectrum and SEM images of the ZnO grown on immobilized gelatin onto a Si substrate at 37 °C in pH 8 buffer for 4 h: (b) cross section tilted 20° and (c) perpendicular to the surface.

constant. The negatively charged oxygen atoms formed from the deprotonated water are then combined with the zinc cations, building the ZnO up.

An experiment was performed to check if gelatin immobilized on a rigid substrate would also behave as an organic matrix by inducing the formation of a ZnO film. The gelatin was covalently immobilized on silicon substrates. The thickness of the gelatin film was calculated as 1.289 nm by AFM experiments after making thin scratches with a sharp tweezers and the average root-mean-square roughness as 0.688 nm (images not shown here). ZnO was crystallized onto the protein coating (Figure 7b,c) using the same experimental conditions as previously excluding obviously the dissolved gelatin. The silicon wafer was placed vertically in a closed chamber during the experiments to avoid any accumulation of ZnO precipitate on its surface. The immobilization of relatively large biomolecules on solid substrates without loss of structural integrity and functionality is one important concern. We could not prove that the method used by us for the protein immobilization retained the three-dimensional structure of the gelatin. But it is confirmed that the gelatin induces the ZnO crystallization even when immobilized. The ZnO layer formed is limited to one particle thick, very rough, and not very compact. When the silicon substrate was not covered with gelatin, very few and much smaller ZnO particles were found on it (results not shown here). The XRD spectrum of the ZnO film in Figure 7a shows a textured (002)-oriented ZnO wurtzite peak. The extra peak with 2θ placed at about 33° corresponds to the silicon substrate.

Conclusion

Gelatin has a big influence on the morphology of ZnO crystalline obtained in aqueous solution at 37 °C and neutral pH. By the presence of dissolved gelatin at a concentration of 0.12 wt %, the particle size of the ZnO changes from approximately 20 nm (in the absence of gelatin) to about 460 nm in diameter. The morphology of this ZnO also changes from round-shaped to twin hexagonal platelets. The gelatin is a soluble macromolecule, which acts as an organic template nucleating the mineralization of ZnO. This adsorption process leads to preferential growth of the crystal's faces, shaping its crystal habit.

Acknowledgment. We gratefully acknowledge Sabine Kühnemann and Hartmut Labitzke for the SEM images, Martina Thomas for the XRD spectra, Wilfried Sigle, Peter Kopold, and Kersten Hahn for the TEM analyses, Ulrike Eigenthaler for the preparation of samples by FIB, Maria Sycha for embedding the sample in resin and microtoming, Ulrike Täffner for the AFM experiments, Stefanie Wildhack for the zeta potential measurements, and Peter Gerstel for laboratory assistance.

Supporting Information Available: Depth image of ZnO cyrstallite taken by TEM and SAED pattern of the (002) exposed face (JPEG) and caption for the figure (PDF). This material is available free of charge via the Internet at http://pubs.acs.org.

CM052317+